New Phytologist

The carrier AUXIN RESISTANT (AUX1) dominates auxin flux into Arabidopsis protoplasts

Heidi L. Rutschow[1,2], Tobias I. Baskin[1] and Eric M. Kramer[2]

[1]Biology Department, University of Massachusetts, Amherst, MA 01003, USA; [2]Physics Department, Bard College at Simons Rock, Great Barrington, MA 01230, USA

Author for correspondence:
Eric M. Kramer
Tel: +1 413 528 7476
Email: ekramer@simons-rock.edu

Received: *18 May 2014*
Accepted: *15 June 2014*

New Phytologist (2014) **204:** 536–544
doi: 10.1111/nph.12933

Key words: *Arabidopsis thaliana*, AUXIN RESISTANT (AUX1), cell sorting, diffusion, indoleacetic acid (IAA), protoplasts, transport.

Summary

- The ability of the plant hormone auxin to enter a cell is critical to auxin transport and signaling. Auxin can cross the cell membrane by diffusion or via auxin-specific influx carriers. There is little knowledge of the magnitudes of these fluxes in plants.
- Radiolabeled auxin uptake was measured in protoplasts isolated from roots of *Arabidopsis thaliana*. This was done for the wild-type, under treatments with additional unlabeled auxin to saturate the influx carriers, and for the influx carrier mutant *auxin resistant 1* (*aux1*). We also used flow cytometry to quantify the relative abundance of cells expressing AUX1-YFP in the assayed population.
- At pH 5.7, the majority of auxin influx into protoplasts – 75% – was mediated by the influx carrier AUX1. An additional 20% was mediated by other saturable carriers. The diffusive influx of auxin was essentially negligible at pH 5.7.
- The influx of auxin mediated by AUX1, expressed as a membrane permeability, was $1.5 \pm 0.3\ \mu m\ s^{-1}$. This value is comparable in magnitude to estimates of efflux permeability. Thus, auxin-transporting tissues can sustain relatively high auxin efflux and yet not become depleted of auxin.

Introduction

The plant hormone auxin (indoleacetic acid (IAA)) plays a role in the regulation of nearly every aspect of growth and development. Key to its many functions is the fact that auxin is transported cell to cell by at least three families of auxin-specific carrier proteins: the ATP-BINDING CASSETTE B (ABCB) family of carriers, the PIN-FORMED (PIN) family of auxin efflux carriers, and the AUXIN RESISTANT 1/LIKE AUX1 (AUX1/LAX) family of influx carriers (Zazimalova *et al.*, 2010). These proteins transport auxin synthesized in one part of the plant to act on cells that are millimeters or even centimeters distant. They also allow auxin to be efficiently segregated between tissues, so that auxin transport and signaling are both strongly tissue-specific (Kramer, 2004; Brunoud *et al.*, 2012).

The basic model of auxin movement is called 'polar auxin transport' (Kramer & Bennett, 2006). It depends in part on the fact that the apoplastic pH is weakly acidic, while the cytosol is near-neutral (Fasano *et al.*, 2001). In the apoplast, a fraction of the auxin molecules are protonated (IAAH) and therefore membrane-permeable, while virtually all the auxin molecules in the cytosol are ionized (IAA−) and membrane-impermeable. Apoplastic auxin can enter a cell in two ways: via influx carriers or by diffusion of its protonated form through the membrane. However, once inside the cell, ionized auxin can exit only via efflux carriers. The polar localization of efflux carriers in a tissue results in the polar cell-to-cell flux of auxin (Wisniewska *et al.*, 2006; Kramer *et al.*, 2011).

Besides long-distance transport, the characterization of auxin carriers in the last 15 yr has revealed a diversity of additional phenomena. During plant development, feedbacks between PIN polarity and auxin concentration in a tissue can result in localized auxin maxima that trigger the development of new meristems (Reinhardt *et al.*, 2003; Dubrovsky *et al.*, 2008) or new vascular tissues (Sauer *et al.*, 2006; Bayer *et al.*, 2009). Studies have also revealed important roles for influx carriers, which function to sequester auxin in specific cells or tissues (Swarup *et al.*, 2005, 2008).

Considering that auxin transport and accumulation both depend critically on influx across the plasma membrane, it is perhaps surprising that the relative contributions attributable to diffusion and influx carriers remain largely uncharacterized. The function of various auxin carriers has been probed by assaying the uptake and efflux of radio-labeled IAA in tissues, cell cultures, and heterologous systems (Loper & Spanswick, 1991; Delbarre *et al.*, 1994, 1996; Geisler *et al.*, 2005; Petrasek *et al.*, 2006; Yang *et al.*, 2006; Yang & Murphy, 2009; Hosek *et al.*, 2012). However, the use of these assays to estimate numerical values for the influx *in planta* is rarely attempted. In addition, there are apparently no reports of influx measurements where the relative contributions of different carriers were distinguished. This has hampered the quantitative understanding of auxin transport and its predictive modeling.

Here, we quantified the diffusive and carrier-mediated influx of auxin in *Arabidopsis thaliana* roots. We used a protoplast system, as this allowed us to precisely control the external auxin

concentration, as compared with tissues or organs, where the auxin environment of each cell is determined by the transport activity of neighboring cells. The heterogeneity of our protoplast suspensions was accounted for using microscopy to measure the range of cell sizes, and by using flow cytometry to measure the fraction of AUX1-positive protoplasts. This allowed us to measure influx for a specific auxin carrier.

Materials and Methods

Plant growth and protoplast preparation

Arabidopsis thaliana L. (Heynh) seeds were surface-sterilized with 25% bleach for 10 min, rinsed three times with sterile water, and held at 4°C for 48 h. Stratified seeds were plated on modified Hoagland's medium (as described in Baskin & Wislon, 1997) and grown vertically for 14 d in constant light (*c.* 100 μmol m^{-2} s^{-1}) and temperature (*c.* 22°C). All material was in the Columbia background. The line expressing tagged AUX1 (*proAUX-AUX-YFP*), described previously (Swarup *et al.*, 2004), was the generous gift of Malcolm Bennett (University of Nottingham, Nottingham, UK). The lines *proPIN1:PIN1-GFP*, *proPIN2:PIN2-GFP*, and *aux1-22* were obtained from the Arabidopsis Biological Resource Center (ABRC; Columbus, OH, USA).

To make protoplasts, roots from 14-d-old plants were removed from plates and placed in a plasmolysis solution (0.5 M mannitol and 20 mM $CaCl_2$) for 1 h. They were then placed in a solution for digestion containing 0.5 M mannitol, 0.1% bovine serum albumin (BSA), 5 mM $CaCl_2$, 5 mM MES buffer, pH 5.7, 5 mM KCl, 0.4% Cellulase-RS (Yakult, Tokyo, Japan), and 0.1% Pectolyase-Y23 (GoldBiotechnology, St Louis, MO, USA). Roots were digested in the dark at room temperature for 4 h. The digest solution was next filtered through a 40-μm mesh strainer (BD Biosciences, San Jose, CA, USA) and then through 22–25-μm Miracloth (EMD Millipore, Billerica, MA, USA). The cell suspension was spun down at 100 ***g*** for 7 min, washed with modified wash buffer (154 mM NaCl, 62.5 mM $CaCl_2$, 5 mM KCl, 2 mM MES, pH 5.7, 2 mM $MgCl_2$, 10 mM glucose and 0.5 M mannitol) (Yoo *et al.*, 2007) and spun again at 100 ***g*** for 7 min. The supernatant was removed and protoplasts were re-suspended in *c.* 1 ml of fresh wash buffer and counted on a hemacytometer.

Uptake assay

After the cell concentration had been determined, cells were diluted to the desired concentration in wash buffer and incubated for *c.* 1 h in 10 μM tri-iodobenzoic acid (TIBA) to suppress auxin efflux, before assaying uptake. For uptake assays, cells were separated into 1.25-ml aliquots. At time zero, 10 nM [5-^{3}H(N)]-indoleacetic acid (Perkin Elmer, Waltham, MA, USA; *c.* 25 Ci $mmol^{-1}$) was added to each aliquot. At each time-point, 250 μl was collected on Whatman GF/A glass microfiber filters (Fisher Scientific, Atlanta, GA, USA) under the vacuum from a water aspirator. Filters were washed with 2 ml of wash buffer, immediately placed in scintillation fluid (Research Products International, Mount Prospect, IL, USA), and counted the next day (LS 6500; Beckman Coulter, Brea, CA, USA). Counts were converted to mmol [^{3}H-IAA] based on the specific activity. Cell-free assays were performed in parallel to determine nonspecific binding to the filters. The mean of these nonspecific counts was subtracted as background.

Flow cytometry

Protoplasts were prepared as described in the section 'Plant growth and protoplast preparation', except that the digestion period was for 14 h. After washing, cells were incubated for 10 min in 10 μM propidium iodide (PI) and then run through a flow cytometer (BD LSRII; BD Biosciences, San Jose, CA, USA). The PI was used as an assay for cell viability. Protoplasts with disproportionately high red signals, *c.* 5% of the total, were presumed dead and excluded from further analysis. Photomultiplier settings were kept the same for each experiment, allowing comparison across runs. For each experiment, at least 30 000 cells were counted for each genotype.

pH dependence of uptake

We estimated the pH dependence of auxin uptake using curve fits to the data in fig. 9 of Loper & Spanswick (1991) and fig. 3(A) of Yang *et al.* (2006). Data points were extracted using ImageJ v1.43 (http://imagej.nih.gov/ij/). The curve fit was made using Kaleidagraph v4.1 (Synergy, Reading, PA, USA) and a phenomenological curve fit equation of the form $f(\mathrm{pH}) = c_0 \exp(c_1 \mathrm{pH} + c_2 \mathrm{pH}^2 + c_3 \mathrm{pH}^3)$, where c_i are four fit parameters.

Results

Validating the protocol

We used root protoplasts of *A. thaliana* to quantify auxin uptake. In our assay, tritiated auxin is added to a suspension of protoplasts at time zero and aliquots are removed at desired times and separated from the medium by vacuum filtration. Radioactivity in the collected material is counted and converted to a cellular concentration of auxin.

Because of concerns that auxin would saturate the influx carrier or trigger physiological changes, the exogenous concentration of labeled auxin was chosen to be as low as possible while still providing enough disintegrations to yield statistically valid results. A concentration of 10 nM IAA resulted in a signal that was reliably above background and still within the physiological range of intercellular IAA (we show in the next section that the influx carriers saturate at a concentration two orders of magnitude higher than this). Because the measured cellular concentration of radiolabeled auxin would typically reflect the net balance of uptake and efflux, we included an inhibitor of auxin efflux, tri-iodobenzoic acid (TIBA), in the protoplast medium. We found that adding TIBA to the uptake medium approximately tripled label retention by protoplasts in auxin for 8 min (retention with 10 μM TIBA: 843 ± 144 zmol ^{3}H-IAA per cell; retention with

no TIBA: 300 ± 96 zmol ^{3}H-IAA per cell; mean ± SEM, $n = 3$), confirming that TIBA inhibits efflux in this system.

One important question is the degree to which protoplasts from root cells retain their auxin transport activities. The transcript profiling data of Birnbaum *et al.* (2003) suggest that protoplasting does not significantly change the transcript levels of known auxin carriers. Here, we further addressed this question by comparing images of fluorescent AUX1-YFP in whole roots and protoplasts (Fig. 1a,b). Both preparations have a qualitatively similar pattern of fluorescence. In the protoplasts, the majority of the signal remains at the plasma membrane and the overall intensity remains high. This contrasts with PIN1-GFP and PIN2-GFP, which in protoplasts lose their preferential localization to the plasma membrane (Fig. 1c,d). The loss of PIN localization from the plasma membrane might be attributable to stress during protoplasting (Nakayama *et al.*, 2012) or because the cell wall is needed for stable localization. The latter possibility is suggested by the observation that PIN1-GFP in tobacco BY-2 cells remains on the plasma membrane immediately after protoplasting (Boutté *et al.*, 2006). Thus, in root protoplasts, influx is plausibly maintained at levels comparable to those found in the root, while efflux is likely to be diminished. Indeed, an inhibitory effect of protoplasting on auxin efflux was previously reported (Petersson *et al.*, 2009).

The majority of IAA uptake is carrier-mediated

In *A. thaliana* root protoplasts, auxin uptake for the first 2 min was approximately linear, followed by a decrease in uptake rate at later times (Fig. 2). The linearity for the first 2 min implies uptake without complicating factors. The decrease in uptake rate at later times was probably attributable to a gradual equilibration between influx and efflux (Hosek *et al.*, 2012), although the absence of a clear plateau means we cannot rule out a role for auxin-induced changes in the protoplasts (e.g. altered cytosolic pH or carrier activity). To avoid these uncertainties, our quantitative analysis focused on the uptake curve at early times.

To determine how much of the uptake was carrier-mediated, we supplemented the incubation medium with unlabeled (i.e. 'cold') IAA, intended to saturate the influx carriers. At the 2 min mark, 1 μM cold IAA reduced the uptake rate by *c.* 75% and 10 μM cold IAA reduced it by *c.* 90%. This result is broadly consistent with the half-saturation constants measured for the uptake carriers AUX1 and LAX3, both being *c.* 850 nM (Yang *et al.*, 2006; Swarup *et al.*, 2008). As diffusive uptake of IAAH across the lipid membrane does not saturate, this suggests that

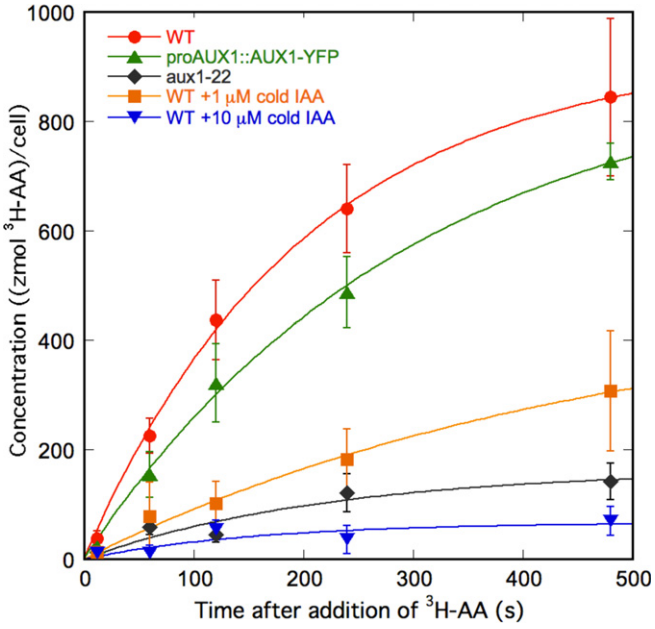

Fig. 2 Uptake of ^{3}H-IAA in *Arabidopsis thaliana* root protoplasts. At time $t = 0$, 10 nM ^{3}H-IAA was added to the suspension medium. Aliquots were then sampled at the times indicated. Uptake is expressed on a per cell basis for wild-type (WT; with additional 0, 1, and 10 mM unlabeled IAA), *aux1-22*, and proAUX1:AUX1-YFP expressed in the *aux1-22* background. Error bars, ± SEM, with $n = 13$, 5, 5, 3 and 7, respectively, from the top to the bottom of the figure. Lines are guides to the eye. The medium included 10 μM tri-iodobenzoic acid (TIBA) to inhibit auxin efflux.

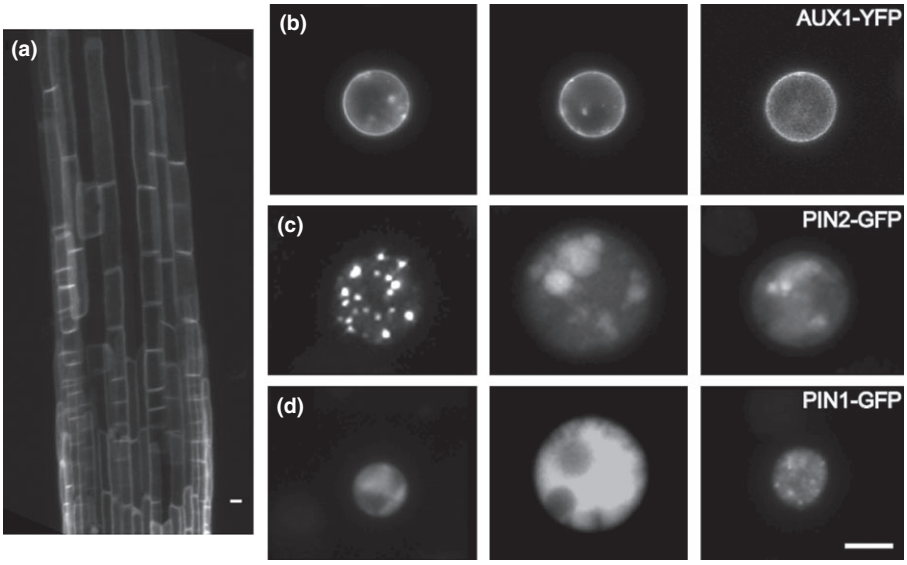

Fig. 1 Carrier localization in *Arabidopsis thaliana* roots and protoplasts. (a, b) Confocal microscope images showing membrane localization of AUX1-YFP in (a) an intact proAUX1:AUX1-YFP root and (b) isolated root protoplasts. (c, d) Confocal microscope images of protoplasts showing cytoplasmic localization of (c) PIN2-GFP and (d) PIN1-GFP. Bars, 10 μm. Abbreviations: AUX1, auxin influx carrier AUXIN RESISTANT 1; PIN, auxin efflux carrier family PIN-FORMED.

carrier-mediated uptake constitutes *c.* 90% of the auxin influx in our system. This analysis will be made more precise in the following sections.

In *A. thaliana*, recognized auxin influx carriers include the four members of the AUX1/LAX family (Péret *et al.*, 2012) and at least two ABCB carriers (Terasaka *et al.*, 2005; Kamimoto *et al.*, 2012; Kubes *et al.*, 2012). We focus on the contribution from AUX1, because it is the most thoroughly studied carrier, and required for root gravitropism (Bennett *et al.*, 1996). To quantify the contribution to auxin influx made by the AUX1 carrier, we assayed uptake in protoplasts derived from *aux1-22*, a partial loss-of-function mutant. Strikingly, uptake into root protoplasts from *aux1-22* was reduced by *c.* 80% as compared with wild-type (Fig. 2). This reduction was comparable in magnitude to the reduction imposed by saturating concentrations of cold IAA, which implies that most of the saturable influx took place via AUX1. In other words, AUX1 was the predominant auxin influx carrier in our protoplasts.

Measuring the relative abundance of AUX1-positive cells

To determine the proportion of root cells that expressed AUX1, we used flow cytometry. We took advantage of a line in which AUX1-YFP is expressed under its native promoter in the *aux1-22* background (Swarup *et al.*, 2004). In the uptake assay described in the previous section, root protoplasts from this line had an uptake rate that was less than, but still comparable to, that of wild-type (Fig. 2). Plotting the intensity of red fluorescence (from propidium iodide) versus green fluorescence (from AUX1-YFP) revealed a population of YFP-positive cells in the transgenic line that were not present in the wild-type protoplasts (Fig. 3). The gate used to count AUX1-positive cells was selected using the green channel, and chosen to exclude at least 98% of the wild-type protoplasts. AUX1-YFP cells with a green-channel intensity greater than this threshold were counted as AUX1-positive. Repeating this in independent experiments gave consistent results, with an average value for the AUX1-positive protoplast fraction of 35% ± 5% (SEM, $n = 5$).

Permeability of the plasma membrane to IAA

To facilitate comparisons between experiments, it is convenient to re-express the influx in terms of a membrane permeability. In the case of negligible efflux, the equation defining permeability is $J = P\,C_{ext}$, where J is the flux entering the cell, C_{ext} is the external auxin concentration, and P is the membrane permeability. The units of flux are moles per unit membrane area per unit time, so the units of permeability are $\mu m\ s^{-1}$. The total amount of labeled auxin accumulating in one protoplast, L, is then a linearly increasing function of t, the time elapsed since the addition of label to the medium:

$$L = A\,P\,C_{ext}\,t \qquad \text{Eqn 1}$$

where A is the surface area of a spherical protoplast (i.e. $4\pi R^2$, where R is the radius).

At early times ($t \leq 120$ s), uptake of radiolabeled IAA into protoplast suspensions was evidently linear with time, but the use of

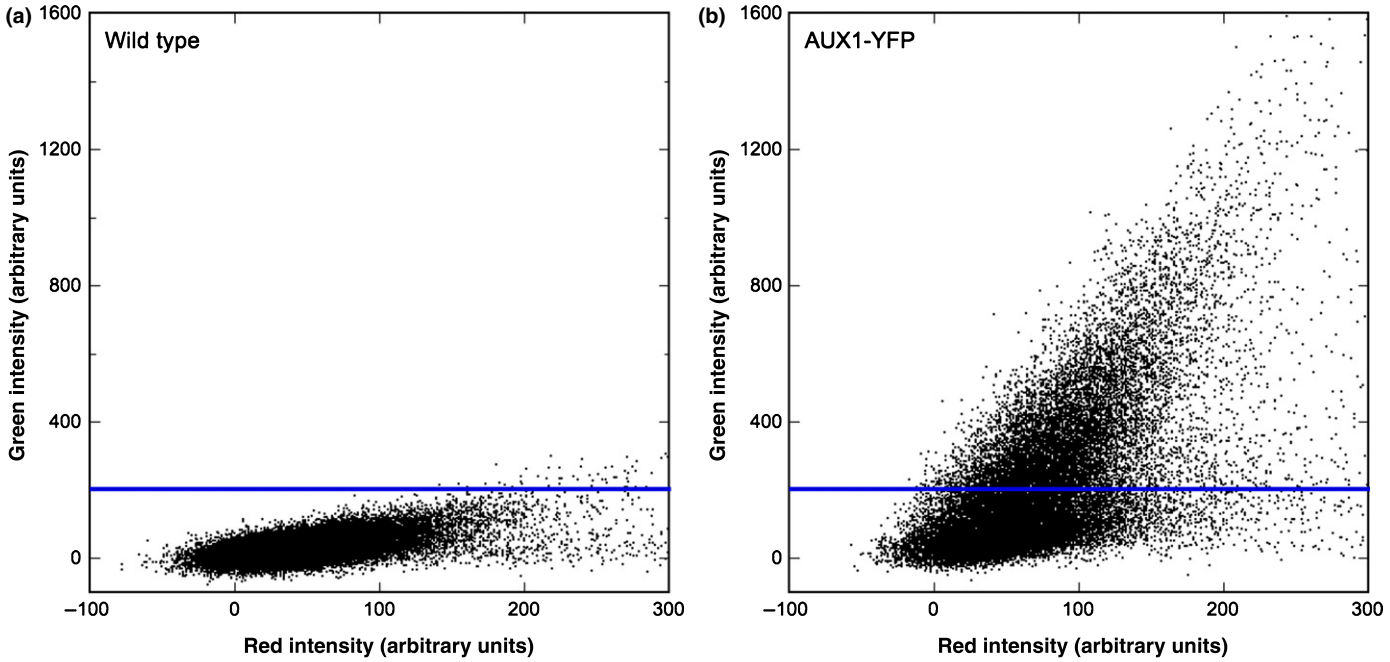

Fig. 3 Flow cytometry assay for AUX1 content. (a, b) Representative plots of green versus red channel intensities for *Arabidopsis thaliana* protoplasts derived from roots of (a) wild-type and (b) proAUX1::AUX1-YFP. Cells were subjected to flow cytometry after staining with propidium iodide. Cells with green intensity greater than that indicated by the blue line were taken as AUX1-YFP positive. $N = 30\,000$ cells for each genotype. The red channel is PE-Texas Red-A. The green channel is AlexaFluor488-A. The average background noise level has been subtracted from both channels, so some dim cells have negative values (Herzenberg *et al.*, 2006). Abbreviations: AUX1, auxin influx carrier AUXIN RESISTANT 1.

Eqn 1 is nontrivial because of the heterogeneity of the protoplast population. In our samples, there was a range of carrier expression levels (and hence permeabilities) and cell radii. We accounted for this heterogeneity by using averages, as follows. Eqn 1 can be written as: $L_i = (4\pi R_i^2) P_i C_{ext} t$, where the i subscript denotes parameters for an individual protoplast. Then, summing over all N protoplasts in the population gives the total accumulated label, L_{tot}, as

$$L_{tot} = \sum_{i=1}^{N} (4\pi R_i^2) P_i C_{ext} t \qquad \text{Eqn 2}$$

and this sum can be rewritten as an average

$$L_{tot} = 4\pi N \langle R^2 P \rangle C_{ext} t \qquad \text{Eqn 3}$$

where the angle bracket denotes an average over all protoplasts in the sample.

The heterogeneity of the sample thus enters the calculation only through the term in angle brackets in Eqn 3, $<R^2P>$. This term simplifies if there are no correlations between protoplast radius and permeability, which appears to be approximately true for our system. Flow cytometry showed little or no correlation between the intensity of the AUX1-YFP signal and the forward-scattered signal that provided a measure of cell size (Fig. 4) (Shapiro, 1995). Confocal microscopy of proAUX1:AUX1-YFP protoplasts was generally consistent with these results, showing bright and dim protoplasts at all sizes. Therefore, we assume that radius and permeability are independent, in which case $<R^2P>$ simplifies to $<R^2>$ $<P>$, the product of the average membrane permeability of the protoplast population and the average squared radius. Eqn 3 can then be rewritten as an expression for the average membrane permeability as:

$$\langle P \rangle = \frac{(L_{tot}/Nt)}{4\pi \langle R^2 \rangle C_{ext}} \qquad \text{Eqn 4}$$

where the numerator, (L_{tot}/Nt), is the linear (early-time) slope of the uptake curves plotted in Fig. 2. This slope was determined numerically by fitting a straight line passing through the origin, using χ^2 minimization as described by Bevington (1969) and implemented using MAPLE v.14 (maplesoft.com).

The average squared radius of protoplasts $<R^2>$ was obtained from measurements of protoplast diameter in bright-field micrographs of *c.* 100 protoplasts each, sampled from aliquots during the uptake experiments. The average squared radius was indistinguishable among the studied genotypes and, for the wild-type, was $39.2 \pm 3.2\ \mu m^2$ (SEM, $n = 8$ biological replicates).

The permeability values we obtained were consistent with our earlier discussion of uptake (Fig. 5). We found that uptake in the influx carrier mutant *aux1-22* was reduced by 75% as compared with the wild-type, and uptake with 10 μM cold IAA added to saturate all influx carriers was reduced by 95%. We can therefore ascribe 75% of the measured uptake to AUX1, 20% to other carriers (and also, possibly, to residual AUX1 activity in *aux1-22*), and 5% to diffusion. In other words, diffusive influx was essentially negligible at this pH.

Next, we estimated an average permeability specifically for the AUX1 influx carrier. Subtracting the permeability of *aux1-22*

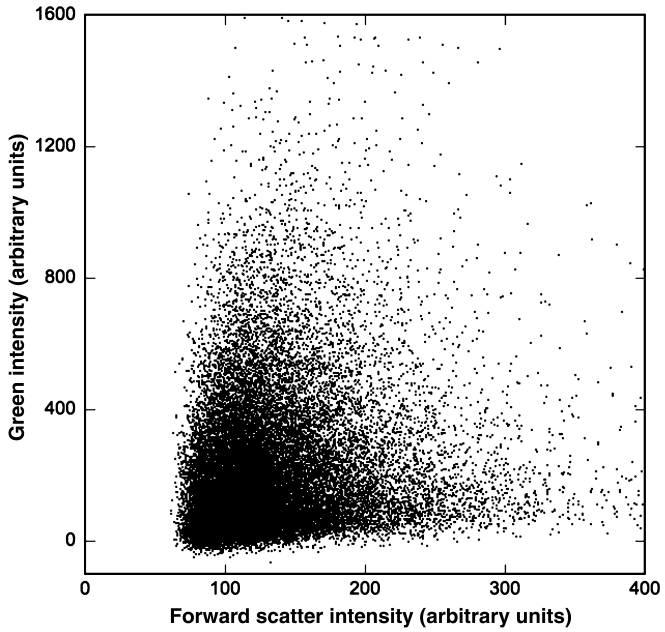

Fig. 4 Flow cytometry analysis comparing AUX1-YFP expression level and cell size in *Arabidopsis thaliana* root protoplasts. Green intensity gives a measure of AUX1-YFP content, and the forward scatter intensity (channel FSC-A) provides an approximate measure of cell volume. $N = 30\,000$ cells, from one representative experiment. Abbreviations: AUX1, auxin influx carrier AUXIN RESISTANT 1.

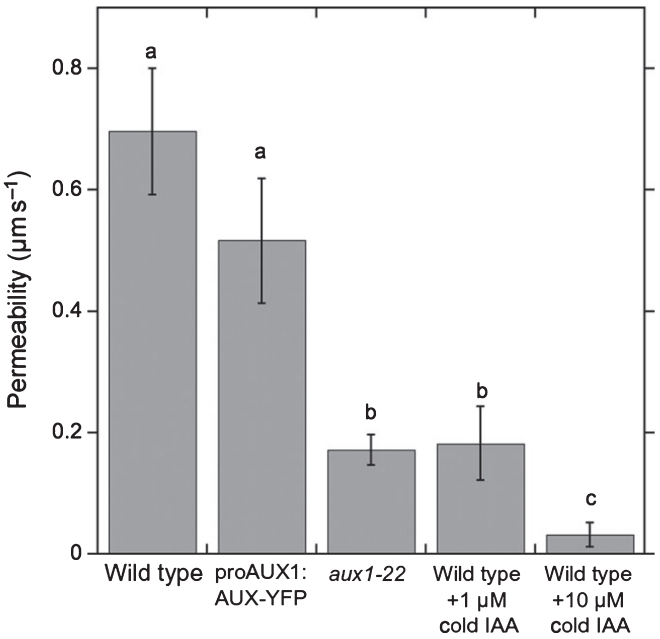

Fig. 5 Auxin uptake permeability in *Arabidopsis thaliana* root protoplasts. Values are for the membrane permeability of ^{3}H-IAA during auxin uptake, calculated for the various experiments shown in Fig. 2. Bars plot mean ± SEM, with $n = 3$ or larger in all cases. Letters distinguish means whose equality is rejected, according to a *t*-test, at $P < 0.05$.

from that of the wild-type gives $P = 0.52 \pm 0.09\ \mu m\ s^{-1}$, an estimate for the permeability attributable to the AUX1 carrier, but averaged over all protoplasts in the suspension. However, our flow cytometry results allow us to adjust this for the fraction of AUX1-positive cells, $f = 35 \pm 5\%$ of the total. Our estimate for the average membrane permeability attributable to the AUX1 carrier in AUX1-positive cells is thus $P_{AUX1} = P/f = 1.5 \pm 0.3\ \mu m\ s^{-1}$.

Permeability as a function of pH

In *A. thaliana* roots, the apoplast ranges from pH 4.5 to 6.0 (Fasano *et al.*, 2001; Monshausen *et al.*, 2011). It is therefore interesting to consider how the permeabilities measured here (at a medium pH of 5.7) will vary as a function of pH.

The diffusive influx of auxin is expected to depend linearly on the fraction of IAA in the protonated form (IAAH), as the anion (IAA−) is membrane-impermeable. The protonated fraction of auxin as a function of pH is $f = 1/(1 + 10^{pH-pK})$, where pK = 4.7 is the acid-base dissociation constant of IAA (Goldsmith *et al.*, 1981). The diffusive permeability of auxin will thus depend on medium pH as

$$P_{diff} = \frac{P_{IAAH}}{1 + 10^{pH-pK}} \qquad \text{Eqn 5}$$

where P_{IAAH} is the permeability of the membrane to IAAH, and P_{diff} is the diffusive permeability one would measure at a given pH. Assuming that the permeability measured at a saturating concentration of 10 μM cold IAA at pH 5.7 represents diffusive influx exclusively (i.e. P_{diff}), then Eqn 5 gives $P_{IAAH} = 0.35 \pm 0.22\ \mu m\ s^{-1}$. This number is in good agreement with prior results: $P_{IAAH} = 0.4\ \mu m\ s^{-1}$ for tobacco leaf protoplasts, and $P_{IAAH} = 0.5\ \mu m\ s^{-1}$ for suspension-cultured tobacco cells (Delbarre *et al.*, 1994, 1996).

Estimating the pH dependence of auxin influx carriers is more complicated. Published measurements of carrier-mediated influx show a broad maximum in uptake rate between pH 5 and 6, and an abrupt decrease in uptake at more basic pH values. Data on the exact location of the uptake maximum are equivocal. Of the two studies of AUX1 in heterologous systems, one shows a peak at pH 5.5 (Carrier *et al.*, 2008), the other near pH 6.0 (Yang *et al.*, 2006). Earlier studies *in planta* do not characterize the carrier type, and generally show an uptake peak closer to pH 5.0 (Rubery, 1978; Loper & Spanswick, 1991). To make an estimate for the variation in uptake as a function of pH, we fitted curves to the uptake data of Loper & Spanswick (1991) and Yang *et al.* (2006), with influx maxima near pH 5 and pH 6, respectively (Fig. 6 inset). These fits predict no more than a factor of 3 variation in P_{AUX1} over the whole physiological range of pH.

Fig. 6 shows the predicted ratio of AUX1-mediated to diffusive influx. We see a large variation in the flux ratio, ranging over nearly two orders of magnitude. This suggests that fluctuations in apoplast pH observed, for example during root acclimation or gravitropism (Fasano *et al.*, 2001; Monshausen *et al.*, 2011), have a significant impact on the distribution of auxin in a tissue.

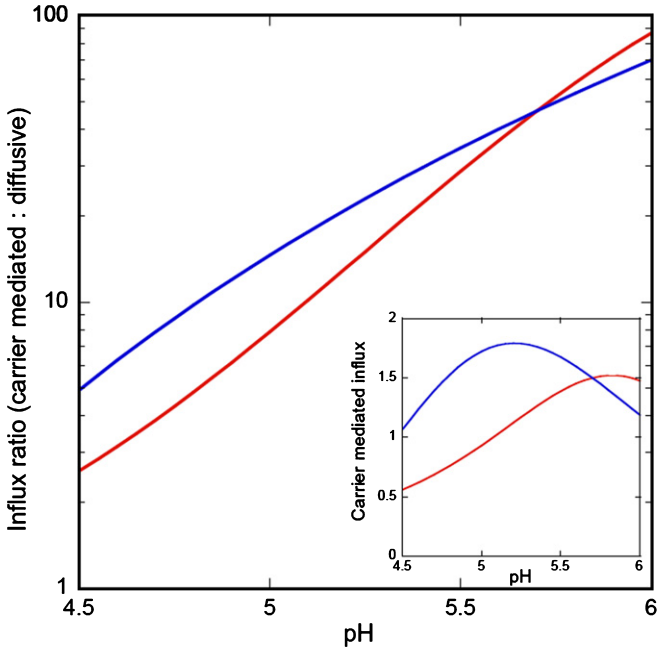

Fig. 6 Influx versus pH. Two estimates are shown for the ratio of carrier-mediated to diffusive auxin influx in AUX1-positive cells of *Arabidopsis thaliana*, using estimates for carrier uptake shown in the inset. Inset: pH dependence of AUX1, estimated using phenomenological curve fits to the data of Loper & Spanswick (1991) and Yang *et al.* (2006); blue and red lines, respectively. Both curves have been normalized to the permeability reported here for AUX1-positive cells, 1.5 μm s^{-1}, at pH 5.7. Abbreviations: AUX1, auxin influx carrier AUXIN RESISTANT 1.

Discussion

In this study we quantified both carrier-mediated and passive diffusion of auxin into *A. thaliana* root protoplasts. Our results allow us to distinguish the action of a single influx carrier, AUX1, from the action of other influx carriers and from diffusive influx. Remarkably, AUX1 accounted for 75% of all the auxin influx in our root protoplast system, with much of the remainder conducted by other saturable carriers. Diffusion accounted for only 5% of the total influx, consistent with earlier work that found a low diffusive permeability for protonated auxin (Delbarre *et al.*, 1996). These values provide a quantitative, as opposed to a qualitative, understanding of auxin fluxes in cells, vital for the construction of accurate models of auxin transport and accumulation within plant tissues.

To better understand the relationship between membrane permeability and cell auxin content, it is helpful to consider a single cell undergoing both auxin influx and efflux. The flux of auxin into the cell is $J_{in} = P_{influx} C_{ext}$, where P_{influx} is the membrane permeability attributable to both carriers and diffusion, and C_{ext} is the external auxin concentration. Similarly, the flux of auxin out may be written approximately as $J_{out} = P_{efflux} C_{in}$, where P_{efflux} is the membrane permeability attributable to efflux carriers and C_{in} is the cytosolic concentration (for the sake of simplicity we will ignore the complicating factors due to polar localization of efflux carriers and the resulting cytosolic auxin gradients). A steady state is achieved when efflux equals influx, $J_{out} = J_{in}$. Rewriting this, we obtain

$$C_{in}/C_{ext} = P_{influx}/P_{efflux} \quad \text{Eqn 6}$$

In other words, the ratio of permeabilities establishes the potential for a cell to accumulate auxin from its environment. The analysis of the steady-state situation in a real plant tissue is complicated by the presence of neighboring cells (Kramer, 2004), but Eqn 6 is a useful first approximation.

Previously, it was pointed out that a file of cells engaged in auxin transport must be able to accumulate auxin from the surrounding tissue, otherwise the efflux carriers will quickly deplete auxin from the file and the auxin flux would be negligible (Kramer, 2004). Cells engaged in transport are therefore expected to have an accumulation ratio C_{in}/C_{ext} comparable to 1 or higher. By Eqn 6, this requires that the influx permeability is comparable to or larger than the efflux permeability.

To estimate the influx-to-efflux permeability ratio in plant cells, we can take advantage of available data for auxin transport speed. The mathematical analysis of an isolated file of model plant cells shows that transport speed is comparable to the efflux permeability, and computer simulations of whole tissues show no major changes to this conclusion (Mitchison, 1980; Goldsmith *et al.*, 1981; Kramer, 2002, 2004). A recent review of published auxin speeds found a wide range of values, 0.5–5 $\mu m\, s^{-1}$, with a median value of 2 $\mu m\, s^{-1}$ (Kramer *et al.*, 2011). We therefore take 2 $\mu m\, s^{-1}$ as an estimate for the efflux permeability of actively transporting cells. Comparing this to the diffusive permeability measured here, on the order of 0.1 $\mu m\, s^{-1}$, we see that diffusive influx alone is insufficient to counteract the depletion of auxin driven by efflux in transporting tissues. This suggests the necessity of auxin influx carriers. Our value for the permeability of AUX1, 1.5 $\mu m\, s^{-1}$, is comparable to our estimate for the efflux permeability, and therefore of the correct magnitude to function in auxin accumulation. It should also be remembered that this is an average value, and that the cells with the highest levels of AUX1 in the root apex will have a larger permeability.

The necessity of influx carriers for the accumulation of auxin within a transporting file has received its clearest validation in the case of AUX1 in the *A. thaliana* root apex. AUX1 is expressed in a continuous layer of cells that passes from the columella to the lateral root cap, and then to the epidermis of the root elongation zone (Swarup *et al.*, 2001). This pathway transmits the asymmetric auxin gradient from the gravity-sensing cells of the columella to the auxin-responsive cells of the elongation zone, and the loss-of-function mutant *aux1* is agravitropic. It was argued in Swarup *et al.* (2005) that the agravitropic phenotype was attributable to a lack of transport competence in the pathway. Our measurements are consistent – auxin diffusion alone is not fast enough to overcome the depletion of auxin by PIN2 efflux carriers in this pathway. The conclusion that AUX1 regulates auxin accumulation in the root apex has recently been validated in Band *et al.* (2014), who found semi-quantitative agreement between observations of a fluorescent auxin reporter construct and a computer model of auxin distribution in the root.

Our results also shed light on the relative importance of AUX1 and other influx carriers in the root. In *A. thaliana*, AUX1 has three paralogs (Péret *et al.*, 2012), and two ATP-binding-cassette transporters, ABCB4 and ABCB21, have also been shown to import auxin (Terasaka *et al.*, 2005; Kamimoto *et al.*, 2012; Kubes *et al.*, 2012). In this study, we measured only the carrier-specific influx for AUX1, but it contributed the majority (75%) of auxin uptake in our system. Perhaps this is why, of the six, only AUX1 was discovered in a mutant screen. We cannot conclude from this that AUX1 is more efficient than the other carriers. Rather, the uptake we observe is a combined effect of carrier permeability, cell size, and the fraction of cells that express a given carrier. The relative importance of these effects for all six influx carriers is a topic for future investigation.

It is interesting to compare our observations with common assumptions about auxin influx found in computer models of plant growth and development. One class of models includes permeabilities similar to those discussed here (e.g. Swarup *et al.*, 2005; Band *et al.*, 2014). These models have historically been used when the pattern of influx carriers is believed to play an important functional role. A second class of models distinguishes carrier-mediated influx from diffusive influx, but with permeabilities that differ from ours in substantial ways (e.g. Wabnik *et al.*, 2010). These models should be treated with caution, although it is possible that the influx permeabilities in aerial tissues are different from those measured here for the root. A third class of models – by far the most common – treat influx as a general property and do not distinguish carrier-positive from carrier-negative cell types (e.g. Grieneisen *et al.*, 2007; Abley *et al.*, 2013). These models will be qualitatively useful, but might miss important features of the auxin partitioning driven by influx carriers.

Lastly, we note that our results suggest that apoplast pH has a key role in regulating auxin distribution between neighboring cells or tissues. Returning to Eqn 6, it is interesting to consider the partitioning of apoplastic auxin between AUX1-positive and AUX1-negative cells. These two cell types will accumulate auxin in the ratio of their influx permeabilities. We pointed out in the previous section that carrier-mediated permeability depends only weakly on pH, while diffusive influx has an exponential dependence on pH. As illustrated in Fig. 5, acidification of the apoplast can increase diffusive influx dramatically, and this would be expected to change the partitioning of auxin between AUX1-positive and AUX1-negative tissues. The importance of pH effects have recently been examined by Steinacher *et al.* (2012), who used a computer model to conclude that apoplastic pH may play a significant role in the regulation of auxin transport. The functional interplay of auxin-triggered acidification and pH-regulated auxin partitioning remains to be explored (Fasano *et al.*, 2001; Monshausen *et al.*, 2011).

Acknowledgements

This work was supported by a grant from the National Science Foundation (grant no. IOS 0815453 to E.M.K. and T.I.B.). Flow cytometry was performed at the UMass Amherst Flow Cytometry Facility with generous assistance from Amy S. Burnside. Thanks also to Elsbeth Walker and Magdalena Bezanilla for helpful discussions regarding uptake assays.

References

Abley K, De Reuille PB, Strutt D, Bangham A, Prusinkiewicz P, Marée AFM, Grieneisen VA, Coen E. 2013. An intracellular partitioning-based framework for tissue cell polarity in plants and animals. *Development* **140**: 2061–2074.

Band LR, Wells DM, Fozard JA, Ghetiu T, French AP, Pound MP, Wilson MH, Yu L, Li W, Hijazi HI *et al.* 2014. Systems analysis of auxin transport in the Arabidopsis root apex. *Plant Cell* **26**: 862–875.

Baskin TI, Wislon JE. 1997. Inhibitors of protein kinases and phosphatases alter root morphology and disorganize cortical microtubules. *Plant Physiology* **113**: 493–502.

Bayer EM, Smith RS, Mandel T, Nakayama N, Sauer M, Prusinkiewicz P, Kuhlemeier C. 2009. Integration of transport-based models for phyllotaxis and midvein formation. *Genes & Development* **23**: 373–384.

Bennett MJ, Marchant A, Green H, May S, Ward S, Millner P, Walker A, Schulz B, Feldmann K. 1996. *Arabidopsis AUX1* gene: a permease-like regulator of root gravitropism. *Science* **273**: 948–950.

Bevington PR. 1969. *Data reduction and error analysis for the physical sciences.* New York, NY, USA: McGraw-Hill.

Birnbaum K, Shasha DE, Wang JY, Jung JW, Lambert GM, Galbraith DW, Benfey PN. 2003. A gene expression map of the Arabidopsis root. *Science* **302**: 1956–1960.

Boutté Y, Crosnier M-T, Carraro N, Traas J, Satiat-Jeunemaitre B. 2006. The plasma membrane recycling pathway and cell polarity in plants: studies on PIN proteins. *Journal of Cell Science* **119**: 1255–1265.

Brunoud G, Wells DM, Oliva M, Larrieu A, Mirabet V, Burrow AH, Beeckman T, Kepinski S, Traas J, Bennett MJ *et al.* 2012. A novel sensor to map auxin response and distribution at high spatio-temporal resolution. *Nature* **482**: 103–108.

Carrier DJ, Bakar NTA, Swarup R, Callaghan R, Napier RM, Bennett MJ, Kerr ID. 2008. The binding of auxin to the Arabidopsis auxin influx transporter AUX1. *Plant Physiology* **148**: 529–535.

Delbarre A, Muller P, Guern J. 1996. Comparison of mechanisms controlling uptake and accumulation of 2,4-dichlorophenoxy acetic acid, naphthalene-1-acetic acid, and indole-3-acetic acid in suspension-cultured tobacco cells. *Planta* **198**: 532–541.

Delbarre A, Muller P, Imhoff V, Morgat J-L, Barbier-Brygoo H. 1994. Uptake, accumulation and metabolism of auxins in tobacco leaf protoplasts. *Planta* **195**: 159–167.

Dubrovsky JG, Sauer M, Napsucialy-Mendivil S, Ivanchenko MG, Friml J, Shishkova S, Celenza J, Benkova E. 2008. Auxin acts as a local morphogenetic trigger to specify lateral root founder cells. *Proceedings of the National Academy of Sciences, USA* **105**: 8790–8794.

Fasano J, Swanson S, Blancaflor EB, Dowd P, Kao T-H, Gilroy S. 2001. Changes in root cap pH are required for the gravity response of the Arabidopsis root. *Plant Cell* **13**: 907–921.

Geisler M, Blakeslee JJ, Bouchard R, Lee OR, Vincenzetti V, Bandyopadhyay A, Titapiwatanakun B, Peer WA, Bailly A, Richards EL *et al.* 2005. Cellular efflux of auxin catalyzed by the Arabidopsis MDR/PGP transporter AtPGP1. *Plant Journal* **44**: 179–194.

Goldsmith MHM, Goldsmith TH, Martin MH. 1981. Mathematical analysis of the chemosmotic polar diffusion of auxin through plant tissues. *Proceedings of the National Academy of Sciences, USA* **78**: 976–980.

Grieneisen VA, Xu J, Maree AFM, Hogeweg P, Scheres B. 2007. Auxin transport is sufficient to generate a maximum and gradient guiding root growth. *Nature* **449**: 1008–1013.

Herzenberg LA, Tung J, Moore WA, Herzenberg LA, Parks DR. 2006. Interpreting flow cytometry data: a guide for the perplexed. *Nature Immunology* **7**: 681–685.

Hosek P, Kubes M, Lankova M, Dobrev PI, Klıma P, Kohoutova M, Petrasek J, Hoyerova K, Jirina M, Zazimalova E. 2012. Auxin transport at cellular level: new insights supported by mathematical modelling. *Journal of Experimental Botany* **63**: 3815–3827.

Kamimoto Y, Terasaka K, Hamamoto M, Takanashi K, Fukuda S, Shitan N, Sugiyama A, Suzuki H, Shibata D, Wang B *et al.* 2012. Arabidopsis ABCB21 is a facultative auxinimporter/exporter regulated by cytoplasmic auxin concentration. *Plant and Cell Physiology* **53**: 2090–2100.

Kramer EM. 2002. A mathematical model of pattern formation in the vascular cambium of trees. *Journal of Theoretical Biology* **216**: 147–158.

Kramer EM. 2004. PIN and AUX/LAX proteins: their role in auxin accumulation. *Trends in Plant Science* **9**: 578–582.

Kramer EM, Bennett MJ. 2006. Auxin transport: a field in flux. *Trends in Plant Science* **11**: 382–386.

Kramer EM, Rutschow HL, Mabie SS. 2011. AuxV: a database of auxin transport velocities. *Trends in Plant Science* **16**: 461–463.

Kubes M, Yang H, Richter GL, Cheng Y, Młodzinska E, Wang X, Blakeslee JJ, Carraro N, Petrasek J, Zazımalova E *et al.* 2012. The Arabidopsis concentration-dependent influx/efflux transporter ABCB4 regulates cellular auxin levels in the root epidermis. *Plant Journal* **69**: 640–654.

Loper M, Spanswick R. 1991. Auxin transport in suspension-cultured soybean root cells: I. Characterization. *Plant Physiology* **96**: 184–191.

Mitchison GJ. 1980. The dynamics of auxin transport. *Proceedings of the Royal Society of London. Series B, Biological Sciences* **209**: 489–511.

Monshausen GB, Miller ND, Murphy AS, Gilroy S. 2011. Dynamics of auxin-dependent Ca2+ and pH signaling in root growth revealed by integrating high-resolution imaging with automated computer vision-based analysis. *Plant Journal* **65**: 309–318.

Nakayama N, Smith RS, Mandel T, Robinson S, Kimura S, Boudaoud A, Kuhlemeier C. 2012. Mechanical regulation of auxin-mediated growth. *Current Biology* **22**: 1468–1476.

Péret B, Swarup K, Ferguson A, Seth M, Yang Y, Dhondt S, James N, Casimiro I, Perry P, Syed A *et al.* 2012. AUX/LAX genes encode a family of auxin influx transporters that perform distinct functions during Arabidopsis development. *Plant Cell* **24**: 2874–2885.

Petersson SV, Johansson AI, Kowalczyk M, Makoveychuk A, Wang JY, Moritz T, Grebe M, Benfey PN, Sandberg G, Ljung K. 2009. An auxin gradient and maximum in the Arabidopsis root apex shown by high-resolution cell-specific analysis of IAA distribution and synthesis. *Plant Cell* **21**: 1659–1668.

Petrasek J, Mravec J, Bouchard R, Blakeslee J, Abas M, Seifertova D, Wisniewska J, Tadele Z, Kubes M, Covanova M *et al.* 2006. PIN proteins perform a rate-limiting function in cellular auxin efflux. *Science* **312**: 914–918.

Reinhardt D, Pesce E, Steiger P, Mandel T, Baltensperger K, Bennett MJ, Traas J, Friml J, Kuhlemeier C. 2003. Regulation of phyllotaxis by polar auxin transport. *Nature* **426**: 255–260.

Rubery PH. 1978. Hydrogen ion dependence of carrier-mediated auxin uptake by suspension-cultured crown gall cells. *Planta* **142**: 203–206.

Sauer M, Balla J, Luschnig C, Wisniewska J, Reinöhl V, Friml J, Benková E. 2006. Canalization of auxin flow by Aux/IAA-ARF-dependent feedback regulation of PIN polarity. *Genes & Development* **20**: 2902–2911.

Shapiro HM. 1995. *Practical flow cytometry.* New York, NY, USA: Wiley-Liss.

Steinacher A, Leyser O, Clayton RH. 2012. A computational model of auxin and pH dynamics in a single plant cell. *Journal of Theoretical Biology* **296**: 84–94.

Swarup K, Benkova E, Swarup R, Casimiro I, Peret B, Yang Y, Parry G, Nielsen E, Smet ID, Vanneste S *et al.* 2008. The auxin influx carrier LAX3 facilitates lateral root emergence. *Nature Cell Biology* **10**: 946–954.

Swarup R, Friml J, Marchant A, Ljung K, Sandberg G, Palme K, Bennett MJ. 2001. Localization of the auxin permease AUX1 suggests two functionally distinct hormone pathways operate in the *Arabidopsis* root apex. *Genes & Development* **15**: 2648–2653.

Swarup R, Kargul J, Marchant A, Zadik D, Rahman A, Mills R, Yemm A, May S, Williams L, Millner P *et al.* 2004. Structure-function analysis of the presumptive Arabidopsis auxin permease AUX1. *Plant Cell* **16**: 3069–3083.

Swarup R, Kramer EM, Perry P, Knox K, Leyser HMO, Haseloff J, Beemster GTS, Bhalerao R, Bennett MJ. 2005. Root gravitropism requires lateral rooot cap and epidermal cells for transport and response to a mobile auxin signal. *Nature Cell Biology* **7**: 1057–1065.

Terasaka K, Blakeslee JJ, Titapiwatanakun B, Peer WA, Bandyopadhyay A, Makam SN, Lee OR, Richards EL, Murphy AS, Sato F *et al.* 2005. PGP4, an ATP binding cassette p-glycoprotein, catalyzes auxin transport in *Arabidopsis thaliana* roots. *Plant Cell* **17**: 2922–2939.

Wabnik K, Kleine-Vehn J, Balla J, Sauer M, Naramoto S, Reinohl V, Merks R, Govaerts W, Friml J. 2010. Emergence of tissue polarization from synergy of intracellular and extracellular auxin signaling. *Molecular Systems Biology* **6**: 447.

Wisniewska J, Xu J, Seifertova D, Brewer PB, Ruzicka K, Blilou I, Rouquie D, Benkova E, Scheres B, Friml J. 2006. Polar PIN localization directs auxin flow in plants. *Science* **312**: 883.

Yang H, Murphy AS. 2009. Functional expression and characterization of Arabidopsis ABCB, AUX 1 and PIN auxin transporters in *Schizosaccharomyces pombe*. *Plant Journal* **59**: 179–191.

Yang Y, Hammes U, Taylor C, Schachtman DP, Nielsen E. 2006. High-affinity auxin transport by the AUX1 influx carrier protein. *Current Biology* **16**: 1123–1127.

Yoo S-D, Cho Y-H, Sheen J. 2007. Arabidopsis mesophyll protoplasts: a versatile cell system for transient gene expression analysis. *Nature Protocols* **2**: 1565–1572.

Zazimalova E, Murphy AS, Yang H, Hoyerova K, Hosek P. 2010. Auxin transporters – why so many? *Cold Spring Harbor Perspectives in Biology* **2**: a001552.